

# Wastewater treatment using Titanium dioxide modified Alumino-Silicate Clay

Ajala, M. A.<sup>1,3</sup>, Abdulkareem A. S.<sup>3</sup>, Tijani, J. O.<sup>2</sup>, Kovo, A.S.<sup>1</sup> Tayo-Alabi A.C.<sup>1</sup>

<sup>1</sup> Department of Chemical Engineering, University of Ilorin, Ilorin.

<sup>2</sup> Department of Chemistry, Federal University of Technology, Minna.

<sup>3</sup> Department of Chemical Engineering, Federal University of Technology, Minna

Corresponding author contact: Email: [ajala.ma@unilorin.edu.ng](mailto:ajala.ma@unilorin.edu.ng), Tel: 08032429560

## Abstract

The removal of heavy metals from wastewater using titanium dioxide modified alumino-silicate clay of Nigerian extract is reported. The clay was beneficiated and characterised. Titanium dioxide was green synthesized with *Parkia Biglobossa* leaf extract. The TiO<sub>2</sub>-clay composite was used to treat wastewater of concentration up to 1000 mg/L of Zn (II) and Pb (II) ions. Effects of adsorbent dose, temperature, contact time, and pH on the percentage Zn (II) and Pb (II) ions removal were evaluated. Kinetics parameter were also determined. Characterization results showed that the clay was thermally stable at temperature up to 800°C, contains functional groups that are suitable for binding up heavy metals and adsorbing other toxic pollutants, and was highly rich in alumina and silica. Results showed that up to 99.00% Zn (II) and 92.51% Pb (II) ions were removed using 20 g/L of adsorbent at 30°C. The pseudo-second order model was the best fit for the adsorption kinetics. These experimental results presented showed that synthesized local clay-titanium nanocomposites are suitable and make good adsorbents for removing heavy metals from industrial wastewater.

## 1. Introduction

In water remediation, there are several technologies that has been studied to improve the process (Morin, 2011; Fu and Wang, 2011; Prasse *et al.*, 2011; Kansara, *et al.*, 2016). Such methods as ordinary filtration, sedimentation, adsorption with several materials, resin, ozonation and reverse osmosis have been considered (Morin, 2011; Fu and Wang, 2011; Prasse *et al.*, 2011; Kansara, *et al.*, 2016). But the assessment of these methods has shown that adsorption process is more favourable as it requires low maintenance, it is economical and energy efficient. Of particular interest is the adsorption of heavy metals because of their toxicity, bioaccumulation, carcinogenicity and non-biodegradability (Gautam *et al.*, 2014; Ksakas *et al.*, 2018).

Extensive studies have been conducted on heavy metals adsorption using several materials ranging from wastes like plant parts, engineered materials like nanoparticles, and naturally abundant materials such as clay (Gautam *et al.*, 2014; Ksakas *et al.*, 2018). Clays have been used for adsorption of several pollutants and adjudged capable and effective for removing heavy metals (Errais *et al.*, 2011). Clays are porous hydro aluminosilicate minerals that make up the colloid fraction of soils, sediments, rocks, with different cavity structure. They have high ion exchange capacity, relatively available in varieties, and act as natural scavengers for heavy metal ions.

Clay materials are comprised of tetrahedral and octahedral layers which have been studied and found to interact with different ions either as a lone adsorbent or impregnated with nanoparticles or activated carbon. The interactions of clay with other adsorbents improves the adsorptive properties with different responses to conditions such as varied contact time, temperature, pH, adsorbent quantity and others (Atkovska *et al.*, 2018). One such adsorbent that could be improved by clay is titanium dioxide which has been widely used for adsorptive wastewater treatment. Titanium dioxide is non-toxic, has high oxidizing properties, it is super hydrophilic and chemically stable (Li *et al.*, 2008; Rossetto *et al.*, 2010; Laysandra *et al.*, 2017). A major drawback of using titanium dioxide in water treatment is its susceptibility to aggregation, thereby reducing its surface area and efficiency. The use of an appropriate clay as support material is able to improve the immobilization of clay particles on the titanium nanoparticles and overcome the shortcoming.

In the current study, local clay was employed as a cheap and available support to immobilize green-synthesized TiO<sub>2</sub> from aqueous leaf extract of *Parkia biglobossa* to adsorb Copper ions, Lead ions and Zinc ions as an alternative adsorbent with high adsorption capacity. The effects of physical parameters such as time, adsorbent dosage, pH and temperature in addition with the kinetics of the adsorption process have been determined.

## 2. Materials and Methods

### 2.1 Materials

Local clay used in this study was obtained from clay deposit in Akerebiata Ilorin. Titanium hydroxide was from JHD, the leaves samples were collected from the premise of University of Ilorin, Kwara State Nigeria.



## 2.2 Synthesis of Titanium Oxide nanoparticles and production of Clay-TiO<sub>2</sub> composites

The leaves of *Parkia biglobosa* (African locust bean) were collected, dried at ambient for 14 days and subsequently ground and sieved to obtain fine powder. The powder was analyzed for its phytochemical composition of phenol, flavonoid and tannin. Next, the whole extract of *Parkia biglobosa* was prepared by adding known weight of its pulverized dried leaves into deionized water in a conical flask and placed on a magnetic stirrer at 50°C for 25 minutes. The leaf extract was obtained by filtering through a filter paper and stored at 4°C prior the time of use. Titanium dioxide nanoparticles were synthesized at a different synthesis parameters of; precursor volume (mL) (from 0.5M Titanium hydroxide standard solution), leaf extract volume (mL) and stirring speed of 2000 rpm for two hours at a pH of 8. A light green colour was obtained with the addition of plant extract into titanium hydroxide solution. After continuous stirring, the colour changed from light green to brown which is an indicator of the formation of titanium nanoparticles (Chatterjee et al., 2016; Sundrarajan and Gowri, 2011). The wavelength of the nanoparticles formed was analysed with Uv-Visible Spectrophotometer. The titanium nanoparticles were acquired by filtration using Whatmann filter paper, then the nanoparticles were washed with deionized water, allowed to age overnight before calcination for 2 hours in a muffle furnace at 450°C temperature.

The synthesis condition for Titanium oxide was used to prepare Clay-Titanium oxide nanoparticle, the slurry was shaken for 2 hours at room temperature, washed, filtered, dried for one hour at 100°C temperature, and then, calcined for two hours in a muffle furnace.

## 2.3 Materials Characterisation

The characterization of titanium nanoparticles obtained was done to determine the wavelength of nanoparticle formation, crystalline size and functional groups attached to the synthesized nanoparticle using methods such as UV- visible spectroscopy, XRD (X-Ray Diffraction) and FTIR (Fourier Transform Infra-Red Spectrophotometry). Ultraviolet-visible spectrophotometer (UV-Vis) model: DU730, Beckman Coulter was used and the sample analysed over 200-700 nm wavelength.

Fourier Transform Infrared Spectroscopic (FTIR) analysis was performed on leaves, clay and TiO<sub>2</sub>-Alumina silicate adsorbent. The spectra of the samples were acquired at a wave number of 4000 to 500 cm<sup>-1</sup>.

X-ray diffraction patterns of the samples were obtained using a Bruker AXS Advance diffractometer with 2θ range of 20 - 90°, a step size of 0.028°, and operating at 45kV and 40 mA. The mean Crystallite size of the nanoparticles (D), were obtained using the Debye-Scherrer equation (1).

$$D = \frac{k\lambda}{\beta \cos \theta} \quad (1)$$

Where  $k$  is a constant ( $k = 0.94$ ), and  $\lambda = 1.54060$ ,  $\theta$  is Bragg angle and  $\beta$  the full width half maximum (FWHM) of the peak at  $2\theta$ .

## 2.4 Collection and Analysis of wastewater

Wastewater was collected from a pharmaceutical company in Ilorin. The wastewater was analysed for heavy metal components and concentrations. Based on this result, wastewater of higher concentration (1000 mg/L) was simulated for the adsorption experiments, in order to ascertain the efficacy of the as prepared adsorbent.

## 2.5 Batch Adsorption Equilibrium Studies

Equilibrium test was carried out on the adsorption of Zn<sup>2+</sup> and Pb<sup>2+</sup> onto aluminosilicate-titanium composite adsorbent prepared. The effect of contact time, adsorbent dosage, pH, and temperature on the adsorption of Zn<sup>2+</sup> and Pb<sup>2+</sup> ions onto the adsorbent were investigated. For the equilibrium studies, the experiment was carried out for 240 minutes so as to ensure that equilibrium was attained. The adsorbent was separated by filtration through whatman filter paper before analysis. The concentration of metal ions before and after adsorption was determined by Atomic Absorption Spectroscopy (AAS) (Buck Scientific Accusys 211 model) in all experiments.

The adsorbed phase concentration ( $q_t$ , in mg/g) at time ( $t$ ) was calculated using the following equation,

$$q_t = \frac{(C_0 - C_t)V}{m} \quad (2)$$

Where,  $C_0$  and  $C_t$  are the initial and the final Lead and Zinc concentration (mg/L) respectively;  $V$  is the water sample volume (L); and  $m$  is the mass of adsorbent used (g).

The adsorption at equilibrium,  $q_e$  (mg/g), was calculated according to Equation (3)

$$q_e = \frac{(C_0 - C_e)V}{m} \quad (3)$$



Where,  $C_0$  and  $C_e$  are the initial and the final (equilibrium) lead/copper concentration (mg/L) respectively;  $V$  is the water sample volume (L); and  $m$  is the mass of adsorbent used (g).

The percentage of lead/copper ion removal was calculated using Equation 4:

$$\text{Removal (\%)} = \frac{C_0 - C_e}{C_0} \times 100\% \quad (4)$$

## 2.6 Effects of Adsorption Parameters

Effects of; contact time (30, 60, 90, 120, 150, 180, 210, 240 minutes), adsorbent dosage (1, 20 g), pH (2, 10), and temperature (30, 40, 50) on the adsorption of  $Zn^{2+}$  and  $Pb^{2+}$  ions onto the Clay-TiO<sub>2</sub> adsorbent prepared were determined by using 0.5 g of adsorbent suspended in 50 mL of 1000 mg/L simulated Cu<sup>2+</sup>- Pb<sup>2+</sup> ions wastewater solution measured into 125 ml Erlenmeyer flask. The flask was agitated at 30°C at a constant 125 rpm using a thermostatic water bath shaker for 240 minutes. The supernatant was filtered and analysed. During the experiment, the particular parameter considered was varied while the other three were kept constant. The adsorbent was separated by filtration through Whatman filter paper. The concentration of metal ions in filtrate was determined by Atomic Absorption Spectroscopy in all experiments.

## 3. Results and Discussion

### 3.1 Phytochemical constituents of *Parkia Biglobbosa*

Phytochemicals	Interference
Tannin	+
Flavonoids	+
Phenol	+
Steroids	+
Phlobatannins	-

Key (+) present (-) absent

The leaves of parkia biglobbosa was analysed and certified to contain phenolic group, tannin and flavonoids which serves as reducing, capping and stabilizing agent, therefore, the *Parkia biglobbosa* leaves is fit for the synthesis of titanium dioxide nanoparticles.

### 3.2 FTIR analysis

The FTIR spectra given in Figure 1 below shows the absorption peaks of *Parkia biglobbosa*, characteristic peaks of O-H stretching vibrations distinctive of phenol group were observed in the range of 3100-3600 cm<sup>-1</sup>. This is confirmed by the peak at 1442.80 cm<sup>-1</sup> of aromatic rings of C=C stretching vibrations in the range of 1400-1450 cm<sup>-1</sup>. The peak at 1026.16 cm<sup>-1</sup> corresponds to C-OH stretching vibrations of aromatics. The peaks at 1627.97 cm<sup>-1</sup> and 1728.28 cm<sup>-1</sup> are attributed to C=O stretching vibrations of esters, ketones and aldehydes. The peaks at 2746.73 cm<sup>-1</sup> and 2862.46 cm<sup>-1</sup> correspond to C-H stretching vibrations of aldehydes. The peaks at 678.97 cm<sup>-1</sup> corresponds to =C-H bending vibrations of alkene while the peaks at 1327.07 cm<sup>-1</sup> and 1373.36 cm<sup>-1</sup> are attributed to C-H bending vibrations of alkane. This indicates that *Parkia biglobbosa* has high residue of alcohol (Phenolic group), esters, aldehydes which are capable of reducing and stabilizing nanoparticles complementing the phytochemical analysis result.

Figure 2 is the FTIR spectral of clay, which shows -OH bend of alcohol, phenols and carboxylic acids between 3700 cm<sup>-1</sup> and 3100 cm<sup>-1</sup>. The peak at 1000 cm<sup>-1</sup> represents a C-C bond of alcohols, esters. At 700 cm<sup>-1</sup> -OH out of plane deformation was observed. Between 500 cm<sup>-1</sup> and 400 is a C-X bond of small residual halo-alkanes and C-N-C bend of amines. These peaks revealed that the local clay possesses the functional groups that have capacity to bind heavy metals to itself.

Figure 3 shows the FTIR spectral of The Clay-TiO<sub>2</sub> produced. The Characteristic peaks of Ti-O stretching bands was observed in the range of 700-875cm<sup>-1</sup>. The peak at 746 cm<sup>-1</sup> characteristic of Ti-O bending vibration which indicates formation of metal oxygen bonding. The absorption peak at 1048 cm<sup>-1</sup> corresponds to stretching and angular deformations of Si-O-Si and Si-O-Al. The band at 1624 cm<sup>-1</sup> corresponds to O-H bending vibration of adsorbed water molecule on the surface. The shift in band results indicate that TiO<sub>2</sub> nanoparticles has been incorporated with the alumina silicate particles.

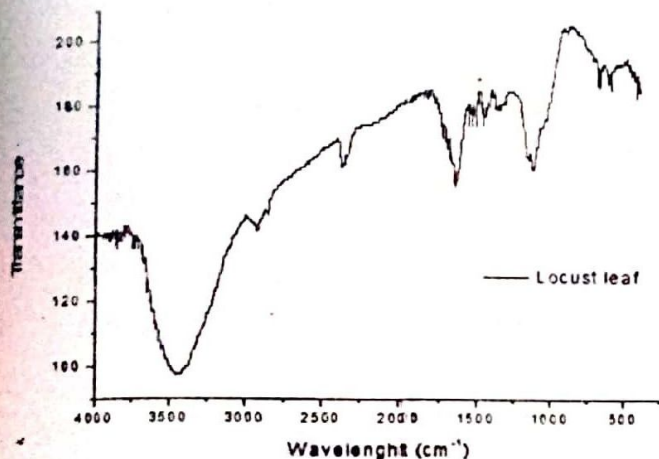


Figure 1: FTIR Spectral of Leaf

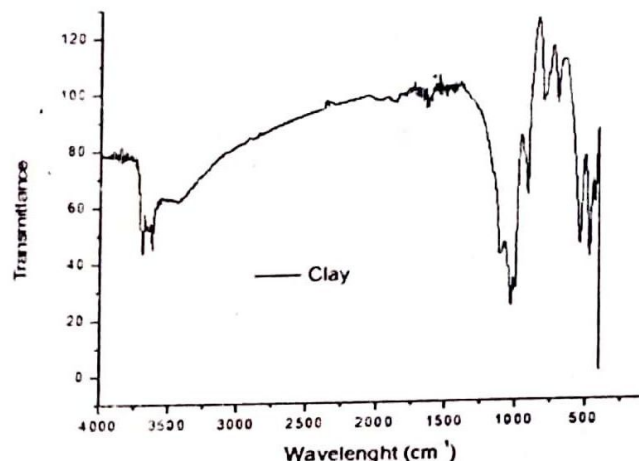


Figure 2: FTIR Spectral of Clay

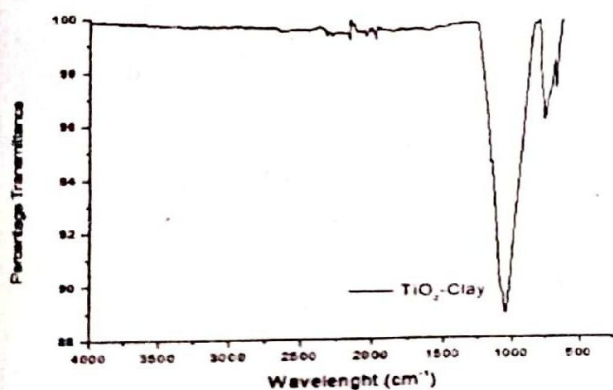


Figure 3: FTIR Spectral of Clay-TiO<sub>2</sub>

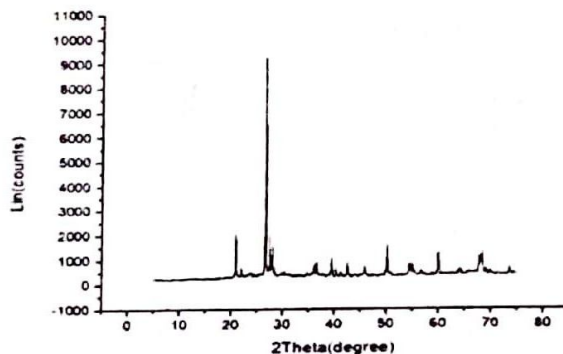


Figure 4: TiO<sub>2</sub>-Clay XRD

### 3.3 XRD Result

The XRD results in figure 4 revealed that the adsorbent is comprised of Aluminium, Silicon and titanium dioxide. The 2 $\theta$  diffraction peak at 20.91° is that of quartz synchronization, an evidence of high silicon dioxide presence, the very sharp peak observed at 26.7°, 2 $\theta$  scale is also of quartz with a crystallite size of 10.28 nm, at 27.50°, 36.11°, 41.2°, 54.92° and 68.38° are titanium (TiO<sub>2</sub>) peaks of rutile transformations, the peaks 28.05°, 36.59°, 39.50°, 51.51°, 59.96°, 67.77° are those of Albite (AlSi<sub>3</sub>O<sub>3</sub>) and Microcline (KAlSi<sub>3</sub>O<sub>8</sub>) synchronizations respectively. The result confirmed the formation of Alumina, Silicate and rutile Titanium dioxide composite.

### 3.4 Effect of contact time

The effect of contact time on the adsorption of Zn (II) and Pb (II) onto TiO<sub>2</sub>-clay is presented in Fig. 5. Varying the time between 30–240 minutes (30 minutes interval), at constant concentration of 1000mg/L, 0.5 g of adsorbent dosage, solution pH, and 30 °C. The percentage adsorption increased steadily from 30 to 90 minutes, when there is no further increase in the percentage ions removal. At this point, equilibrium is ascertained to be reached for both Zn(II) and Pb(II) ions.



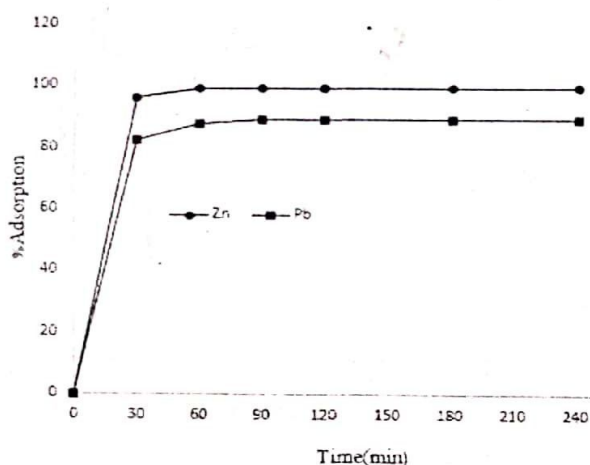


Figure 5. Effect of contact time

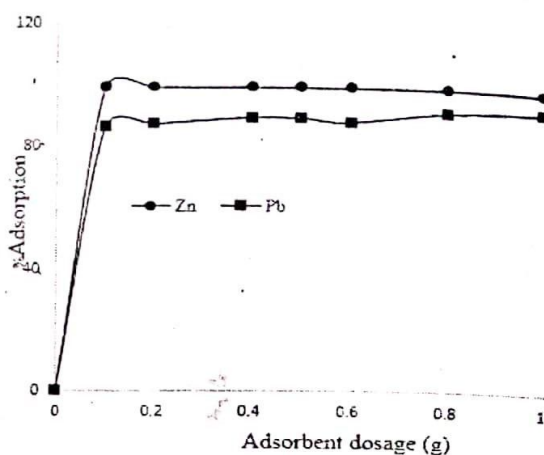


Figure 6. Effect of adsorbent dosage

### 3.5 Effect of adsorbent dosage

Adsorbent dosage is important to determine the adsorption efficiency for a given initial concentration of adsorbate. The data obtained from this experiment is shown in Fig. 5. The increase in adsorbent dosage causes a gradual increase in percentage adsorption for both ions, but, the increase in percentage adsorption of Zn (II) was low as compared to adsorption of Pb (II) as the dosage increases. Zn (II) ion was readily adsorbed with maximum adsorption of 99.00% at 1 g of adsorbent compared to Pb (II) at 92.51%. Therefore, Zn (II) ions has greater affinity for the Clay-TiO<sub>2</sub> adsorbent than Pb (II) ions.

### 3.6 Effect of pH

From Fig. 7, it can be seen that, the increase in pH relatively increased the percentage adsorption for Pb (II). At low pH between 2 and 5, the percentage adsorption is compared low, but increased significantly for pH at 6 and 8. For pH at 10, the percentage adsorption slightly declined, which could be referred to as desorption, which infers that increase in pH above 8 may not be required for effective adsorption of Pb (II) ions. The effect of pH can be seen in the adsorption of Pb (II) where at pH 2, adsorption was obtained as 81.04% and pH 6 was 95.36%. The adsorption (%) for Zn (II) and Pb (II) was highest at pH 8. It can be concluded that the active sites of the adsorbent becomes positively charged at low pH, leading to increase in harmony between H<sup>+</sup> and the positive metal ions for vacant adsorption sites. However, this harmony decreases when the pH increases, as the active sites become more negatively charged with the surface of TiO<sub>2</sub>-clay, which improves the adsorption of the positively charged metal ions by electrostatic force attraction.

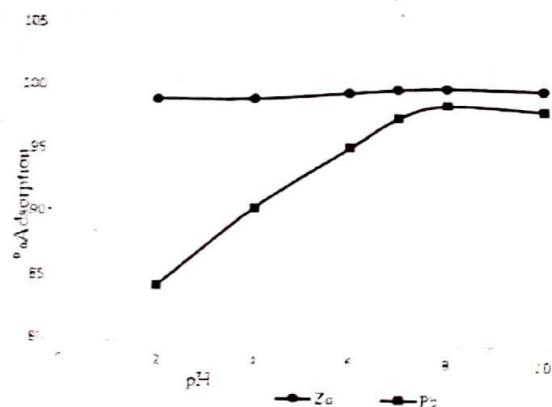


Figure 7. Effect of pH

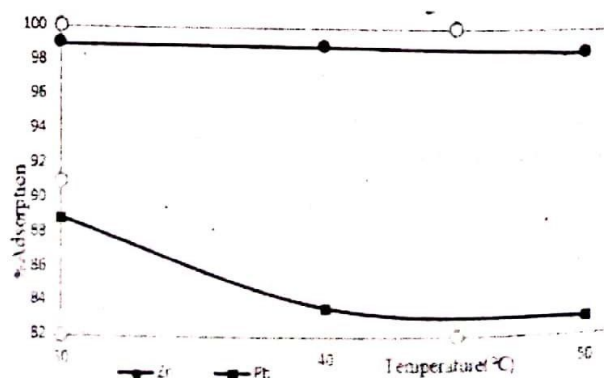


Figure 8. Effect of temperature

### 3.7 Effect of temperature

The effect of temperatures; 30, 40 and 50 °C on the adsorption of Zn (II) and Pb (II) adsorption onto TiO<sub>2</sub>-clay is presented in Fig 8. The study revealed that, percentage adsorption decreased with increase in temperature for Pb (II) ions, but slightly favourable for Zn (II) ions at 40 °C, but worst at 50 °C. Optimum adsorption for both ions was attained at 30 °C with percentage adsorption up to 88.83% Pb(II) and 99.01% for Zn(II).

### 3.8 Adsorption Kinetics

Kinetics and equilibrium of adsorption are the two major parameters to evaluate adsorption dynamics. The kinetic constants of Zn(II) and Pb(II) ions adsorption, which could be used to optimize the residence time of an industrial wastewater treated with TiO<sub>2</sub>-clay, were computed using the experimental data. The adsorption equilibrium was reached at a contact time of 90 minutes.

#### 3.8.1 Pseudo-first order

The adsorption of Zn(II) best fit the model with R<sup>2</sup> value of 0.9993 and R<sup>2</sup> for Pb(II) and Cu(II) at 0.9784. The plot is shown in Figure 9 below. The magnitude of q<sub>e</sub> was in the order of Zn > Pb. The values of q<sub>e</sub> obtained from the plot of the model has wide differences from the experimental values shown in Table 2.

#### 3.8.2 Pseudo-second order

The rate-limiting step is the surface adsorption that involves chemisorption, where the removal from a solution is due to physicochemical interactions. The plot is given by Figure 10 below.

The kinetics of the adsorption of Zn(II) best fit the pseudo-second order with values of R<sup>2</sup> values for Pb(II) as 0.9999 and 0.9999 respectively. This shows that the adsorption is best fit to this model because all the values are close to 1. The fit of the adsorption data to this model indicates that the process is a chemisorption. The values of q<sub>e</sub> obtained from the plot of the pseudo-second order model, presented in Table 2 below is closer to the experimental values.

**Table 2.** Kinetics model parameters for the adsorption process

Heavy Metal	q <sub>e</sub> (mg/g) experiment	Pseudo-first order			Pseudo-second order		
		q <sub>e</sub> (mg/g)	k <sub>1</sub> (min <sup>-1</sup> )	R <sup>2</sup>	q <sub>e</sub> (mg/g)	k <sub>2</sub> (g/mg.min)	R <sup>2</sup>
Zn	99.00	104.48	0.1207	0.9993	99.01	0.0319	1.0000
Pb	89.00	74.71	0.0681	0.9784	89.29	0.0107	0.9999

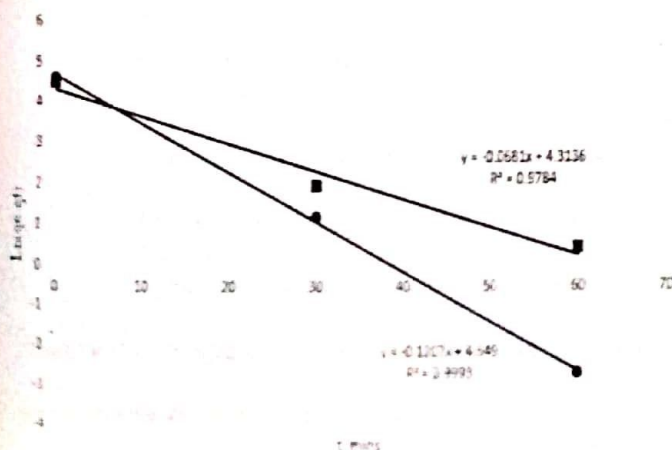
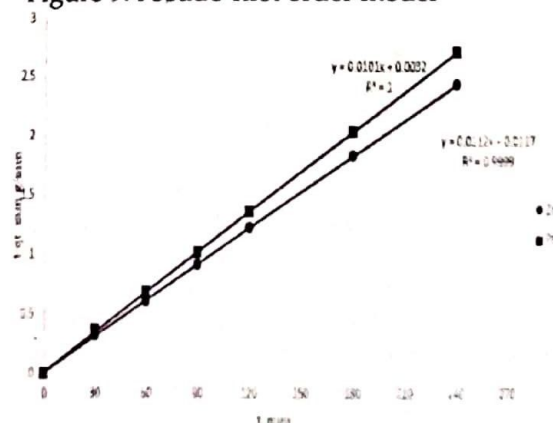


**Figure 10.** Pseudo-second order model

### 4. Conclusion

The leaf extract of *Parkia biglobosa* contain phenols, aldehydes, ketones and esters which are the suitable characteristics of a typical chemical reducing, capping and stabilizing agent. Also, at pH 8, 10g/L adsorbent dosage and 30°C temperature, more than 88% of Zn(II) and Pb(II) ions from 1000mg/L can be removed from

**Figure 9.** Pseudo-first order model





aqueous solution. Therefore, locally sourced, beneficiated alumina silicate clay modified with  $\text{TiO}_2$  has a greater affinity for  $\text{Zn(II)}$  and  $\text{Pb(II)}$  adsorption and is advantageous for potential industrial applications.

## REFERENCES

- Atkovska, K., Lisichkov, K., Ruseska, G., Dimitrov, A. T., and Grozdanov, A. (2018). Removal of heavy metal ions from wastewater using conventional and nanosorbents: A Review. *Journal of Chemical Technology and Metallurgy*, 53(2).
- Chatterjee, A., Nishanthini, D., Sandhiya, N., and Abraham, J. (2016). Biosynthesis of titanium dioxide nanoparticles using *Vigna radiata*. *Asian Journal of Pharmaceutical and Clinical Research*, 9(4), 85-88.
- Fu, F., and Wang, Q. (2011). Removal of heavy metal ions from wastewaters: a review. *Journal of Environmental Management*, 92(3), 407-418.
- Gautam, R. K., Sharma, S. K., Mahiya, S., and Chattopadhyaya, M. C. (2014). Contamination of heavy metals in aquatic media: transport, toxicity and technologies for remediation. *Heavy Metals in Water: Presence, Removal and Safety*, 1-24.
- Guillaume, P., Chelaru, A., Visa, M., and Lassiné, O. (2018). Titanium Oxide-Clay" as Adsorbent and Photocatalysts for Wastewater Treatment. *Journal of Membrane Science and Technology*, 8(1), 1-11.
- Gupta, V. K., and Ali, I. (2013). *Environmental Water: Advances in Treatment, Remediation and Recycling*. Elsevier Science.
- Ho, Y.-S., and McKay, G. (1999). Pseudo-second order model for sorption processes. *Process biochemistry*, 34(5), 451-465.
- Kansara, N., Bhati, L., Narang, M., and Vaishnavi, R. (2016). Wastewater treatment by ion exchange method: a review of past and recent researches. *Environmental Science: An Indian Journal*, 12(4), 143-150.
- Ksakas, A., Tanji, K., El Bali, B., Taleb, M., and Kherbeche, A. (2018). Removal of  $\text{Cu(II)}$  ions from aqueous solution by adsorption using natural clays: kinetic and thermodynamic studies. *Journal of Materials and Environmental Sciences*. 9(3), 1075-1085.
- Lagergren, S. (1898). About the theory of so called adsorption of soluble substances. *Kungliga Svenska Vetenskaps akademien Handlingar*, 24(4), 1-39.
- Laysandra, L., Sari, M. W. M. K., Felycia Edi Soetaredjo, K. F., Putro, J. N., Kurniawan, A., Ju, Y.-H., & Ismadji, S. (2017). Adsorption and photocatalytic performance of bentonite-titanium dioxide composites for methylene blue and rhodamine B decoloration. *Heliyon*, 3, 1-22.
- Liang, R., Hu, A., Hatat-Fraile, M., and Zhou, N. (2014). Fundamentals on adsorption, membrane filtration, and advanced oxidation processes for water treatment *Nanotechnology for Water Treatment and Purification*. Springer.
- Liang, X., Xu, Y., Sun, G., Wang, L., Sun, Y., Sun, Y., and Qin, X. (2011). Preparation and characterization of mercapto functionalized sepiolite and their application for sorption of lead and cadmium. *Chemical Engineering Journal*. 174(1), 436-444.
- Morin, O. J. (2011). Principles and Practises of Reverse Osmosis-Encyclopedia of Life Support systems. . *Membrane Processes*, 11.
- Poursani, A. S., Nilchi, A., Hassani, A., Shariat, S. M., and Nouri, J. (2016). The synthesis of nano  $\text{TiO}_2$  and its use for removal of lead ions from aqueous solution. *Journal of Water Resource and Protection*, 8(4), 438-448.
- Prasse, C., Stalter, D., Schulte-Oehlmann, U., Oehlmann, J., & Ternes, T. (2015). Spoilt for choice: A critical review on the chemical and biological assessment of current wastewater treatment technologies.. *Water Research*. 87, 237-270.
- Rosseto, E., Petkowicz, D. I., dos Santos, J.H.Z., Pergher, S. B. C. & Penha, F.G. (2010). Bentonites impregnated with  $\text{TiO}_2$  for photodegradation of methylene blue. *Applied Clay Science*, 48, 602-606.
- Santhoshkumar, T., Rahuman, A. A., Jayaseelan, C., Rajakumar, G., Marimuthu, S., Kirthi, A. V., and Kim, S. K. (2014). Green synthesis of titanium dioxide nanoparticles using *Psidium guajava* extract and its antibacterial and antioxidant properties. *Asian Pacific Journal of Tropical Medicine*, 7(12), 968-976.
- Shama, S. A., and Gad, M. A. (2010). Removal of heavy metals ( $\text{Fe}^{3+}$ ,  $\text{Cu}^{2+}$ ,  $\text{Zn}^{2+}$ ,  $\text{Pb}^{2+}$ ,  $\text{Cr}^{3+}$  and  $\text{Cd}^{2+}$ ) from aqueous solutions by using hebbra clay and activated carbon. *Portugaliae Electrochimica Acta*, 28(4), 231-239.
- Sharma, S., Rana, S., Thakkar, A., Baldi, A., Murthy, R. S. R., and Sharma, R. K. (2016). Physical, chemical and phytoremediation technique for removal of heavy metals. *Journal of Heavy Metal Toxicity and Diseases*, 1(2), 3-10.
- Singh, P., Kim, Y. J., Zhang, D., and Yang, D. C. (2016). Biological synthesis of nanoparticles from plants and microorganisms. *Trends in biotechnology*, 34(7), 588-599.
- Sundrarajan, M., and Gowri, S. (2011). Green synthesis of titanium dioxide nanoparticles by *Nyctanthes arbor-tristis* leaves extract. *Chalcogenide Letters*, 8(8), 447-451.
- Wang, X., Guo, Y., Yang, L., Han, M., Zhao, J., and Cheng, X. (2012). Nanomaterials as sorbents to remove heavy metal ions in wastewater treatment. *Journal of Environmental and Analytical Toxicology*, 2(7), 1-7.